KAPL-P-000319
(K99115)

A Simple Kinetic Model of Zircaloy $Zr(Fe,Cr)_2$ Precipitate Amorphization During Neutron Irradiation

D.F. Taylor
H.R. Peters
W.J.S. Wang

July 1999

NOTICE

KNOLLS ATOMIC POWER LABORATORY SCHENECTADY, NEW YORK 12301

Operated for the U.S. Department of Energy
by KAPL, Inc. a Lockheed Martin Company

DISCLAIMER

Portions of this document may be illegible in electronic image products. Images are produced from the best available original document.

A Simple Kinetic Model of Zircaloy $Zr(Fe,Cr)_2$ Precipitate Amorphization during Neutron Irradiation

Dale F. Taylor, H. Richard Peters, and Walter J.S. Yang
Lockheed Martin Corporation
P.O. Box 1072
Schenectady, NY 12301
USA

ABSTRACT

At neutron flux levels typical for Zircaloy fuel cladding in commercial power reactors, there is insufficient thermal energy below about 600°K to maintain long-range order in hexagonal close packed (hcp) $Zr(Fe,Cr)_2$ precipitates, and these Laves-phase intermetallics gradually become amorphous. The transformation is homogeneous with no change in composition at low temperatures, but above 500°K, an amorphous zone containing only 10 at% Fe grows inward from the periphery as Fe moves outward to the adjacent alloy matrix. The shrinking central cores of $Zr(Fe,Cr)_2$ precipitates in Zircaloy-4 remain crystalline, while in Zircaloy-2 these precipitates quickly undergo partial transformation and the low-Fe amorphous front advances into a random mixture of amorphous and crystalline regions, each with the original composition. Above 600°K, the $Zr(Fe,Cr)_2$ precipitates tend to retain both their hcp structure and original chemical composition.

These observations suggest that a dynamic competition between kinetic excitation to an amorphous state and thermal recrystallization makes some fraction of the Fe atoms available for flux-assisted diffusion to the alloy matrix by displacing them from hcp lattice positions into metastable, probably interstitial, sites. With one set of kinetic constants, a simple analytic representation of these processes accurately predicts precipitate amorphization as a function of neutron flux, temperature, and time for either Zircaloy-2 or -4. By implication, over the composition range of interest, hcp $Zr(Fe,Cr)_2$ is most stable thermodynamically with about 33 at% Fe, typical of Zircaloy-2, but amorphous $Zr(Fe,Cr)_2$ has the smallest activation energy for recrystallization with the slightly higher Fe content typical of Zircaloy-4.

PACS: 61.80.Az; 61.80.Hg; 61.82.Bg; 82.20.Pm
Key Words: Zircaloy; Laves phase; neutron flux; amorphous zone; iron depletion

INTRODUCTION

Observations - Gilbert *et al.* [1], Yang *et al.* [2,4] and Griffiths *et al.* [3] first described the amorphization of $Zr(Fe,Cr)_2$ intermetallic precipitates in Zircaloy in 1985. Shortly thereafter, Griffiths *et al.* [5] published results from a comprehensive investigation of the phase instability, decomposition and redistribution of precipitates during neutron irradiation in several different types of reactors over a range of fluences and temperatures. That study included analyses of $Zr(Fe,Cr)_2$ amorphization in both Zircaloy-2 and Zircaloy-4, and provided sufficient data for quantitative modeling. Yang [6] demonstrated that post-irradiation annealing could restore the original composition of amorphous precipitates after recrystallization, established the directional nature of precipitate dissolution, and confirmed that its rate is very slow relative to the amorphous transformation.

There are at least four unique characteristics of $Zr(Fe,Cr)_2$ amorphization in a neutron flux that any comprehensive model must address. To summarize from references [1-6]: 1) a complete amorphous transformation occurs quickly and without change in composition at low temperatures (e.g., 350°K); 2) there is little or no transformation of the hcp crystal structure at high temperatures (e.g., 675°K); 3) between about 500°K and 600°K, an amorphous layer grows inward from the precipitate-matrix interface with a simultaneous loss of Fe from that layer to the matrix; and 4) at these intermediate temperatures, the $Zr(Fe,Cr)_2$ precipitates in Zircaloy-2 rapidly develop a random mixture of amorphous and crystalline volume elements that persists within the diminishing core, while in Zircaloy-4, the core remains crystalline as the amorphous shell advances.

The hcp Laves phase apparently is stable over a wide range of ternary compositions. Shaltiel *et al.* [7] studied stoichiometric Laves-phase compounds containing Zr as possible hydrogen storage materials. They observed that pseudobinary $Zr(Fe_xCr_{1-x})_2$ has the hcp crystal structure for $0.25 \le x \le 0.8$, or 17 at%$\le$[Fe]$\le$53 at%, and is cubic for $x \ge 0.9$. $ZrCr_2$ is also cubic [7], and Yang *et al.* [4] narrowed the low-Fe cubic-hexagonal transition to $0.1 < x < 0.25$ by reporting cubic $Zr(Fe_{0.1}Cr_{0.9})_2$ precipitates in Valloy, ternary Zr-1.2Cr-0.1Fe. Yang and Adamson [8] found metastable cubic $Zr(Fe,Cr)_2$ after β-quenching Zircaloy-4 and brief annealing at 1023°K, but only the hexagonal form was stable after annealing at lower temperatures, or for more than 10 min at 1023°K.

Sinha *et al.* [9] considered hyperstoichiometric hcp $ZrCrFe_{1+z}$ systems that are substoichiometric in Zr for hydrogen storage. Their more structurally explicit representation $Zr_{1-y}(FeCr)_y(Fe_xCr_{1-x})_2$, where $y=z/(z+3)$ and $x=(5z+6)/(4z+12)$, indicates that Fe and Cr occupy Zr lattice sites equally in these special derivatives of the parent compound $ZrCr_2$. Since the number of nearest neighbors for each component remains the same across phase transitions in the stoichiometric Laves-phase compounds [7], the replacement of Zr by Cr in the hcp structure seems inconsistent with their finding that $ZrCr_2$ does not accept excess Cr. Without analytical evidence, it is reasonable to conclude that only Fe can occupy either Zr or Cr lattice sites in the hcp structure. The corresponding representation of compositions that are hyperstoichiometric in Fe and

equi-molar in Zr and Cr would be $Zr_{1-y}(Fe_{Zr})_y(Fe_xCr_{1-x})_2$, where y=z/(z+3) and x=(2z+3)/(2z+6).

The stoichiometric $Zr(Fe_xCr_{1-x})_2$ structures are more likely to form spontaneously in dilute Zr alloys like the Zircaloys. Van der Sande and Bement [10] found an Fe:Cr ratio of 5:2 that precisely reflected the compositions of their somewhat atypical heats of Zircaloy-4. Equivalent to $Zr(Fe_{0.7}Cr_{0.3})_2$ or 47 at% Fe, this is slightly higher than the 40 at% Fe in more typical $Zr(Fe_{0.6}Cr_{0.4})_2$ [4]. In Zircaloy-2, deliberate Ni addition yields an Fe:Cr:Ni alloy ratio of approximately 3:2:1. More than trace amounts of Fe partition to tetragonal $Zr_2(Fe,Ni)$ precipitates, and the Fe:Cr ratio in the Laves phase tends to approach unity, or 33 at% Fe. Chemelle *et al.*[11] reported a composition of approximately $Zr(Fe_{0.45}Cr_{0.55})_2$, or an Fe content of 30 at%. Yang *et al.* [4] found about 27 at%, or $Zr(Fe_{0.4}Cr_{0.6})_2$, in Zircaloy-2 with an Fe:Cr:Ni mass ratio of 2.6:2:1.2.

Yang *et al.* [4] recognized that Fe depletion need not accompany precipitate amorphization, but offered the first clear evidence of maximum amorphous structural stability for a hypostoichiometric composition of about 10 at% Fe. Their concentration profiles indicated a constant Cr/Zr mass ratio, and a lower-limit Fe/Zr mass ratio at the amorphous zone/matrix interface of about 0.1. Griffiths *et al.* [3,5], and later, Griffiths [12] published similar composition-profile data, but ignored the amorphous-zone plateau. Yang [6] measured amorphous-zone Fe concentrations between 7 and 12 at% in a subsequent study of precipitate stability. Garzarolli *et al.* [13] also reported 10 at% Fe in precipitates close to the matrix interface after partial or complete transformation at intermediate temperatures.

Yang [6] found an average Fe/Zr mass ratio of 0.53 in crystalline nuclei, and confirmed a constant average Cr/Zr mass ratio of 0.26 across the crystalline/amorphous interphase. This behavior suggests that Fe is the only element with significant mobility. When Fe alone exits a stoichiometric lattice of specific composition, the restoration of local Zr matrix sites could retain some properties of the initial structure by forming boundaries for new micro-crystallites. Thus, if one mole of $Zr(Fe_fCr_{1-f})_2$ loses z moles of Fe, the general hypostoichiometric representation $ZrCr_{2-2f}Fe_{2f-z}$ would become $(Zr_M)_y \bullet Zr(Fe_xCr_{1-x})_2$, where y=z/(2-z) and x=(2f-z)/(2-z). A residual Fe content of 10 at% then translates into $Zr_M \bullet Zr(Fe_{0.2}Cr_{0.8})_2$ as one possibility for the formal description of amorphous zones surrounding the crystalline $Zr(Fe_{0.6}Cr_{0.4})_2$ centers of typical precipitates in Zircaloy-4. It is interesting that this approach predicts a micro-crystallite composition coincident with the hexagonal-to-cubic transition.

Griffiths *et al.* [5] observed that the neutron flux (E>1.0 MeV) influenced an apparent linear dependence of amorphous-layer width upon fluence. The $Zr(Fe,Cr)_2$ precipitates in Zircaloy-2 transformed at about 20 nm/10^{25} n m^{-2} in the Harwell high-flux test reactor Dido, but only at half that rate in a low-flux commercial pressurized heavy-water (PHWR) reactor. They chose not to include the amorphous-zone widths from Dido in their tabular summary, but did provide numerical results for Zircaloy-4 precipitates from a commercial boiling water reactor (BWR) and pressurized water reactor (PWR) that exhibited the lower fluence-dependence at high flux.

Mechanisms - In 1979, the North-Holland Co. published the proceedings of the Workshop on Solute Segregation and Phase Stability During Irradiation in Volume 83 of the Journal of Nuclear Materials. Subsequent progress in describing amorphization has not spawned an accurate quantitative model for Zircaloy Laves-phase precipitates in a neutron flux. In his review, Schulson [14] observed that crystalline-to-amorphous (C→A) transformations occur only in ordered alloys, and not in elemental metals or random solid solutions. He defined amorphization as the complete rearrangement of atoms into a structure having no long-range periodicity, and concluded that a characteristic critical displacement-per-atom (dpa) level decreases both with decreasing temperature and with increasing mass of the projectile. He offered two earlier theories as possible mechanisms for such fluence-dependence: rapid cooling after local melting by spike temperatures within collision cascades, and exceeding a critical defect concentration through the overlap of displacement cascades.

Wilkes [15] treated the flux as a phase-diagram variable, and characterized amorphization as a dynamic, reversible process: a balance between irradiation disordering and the reversion to thermal equilibrium. Low temperatures would then "freeze in" the amorphous phase, and higher temperatures would require higher irradiation rates to produce and maintain it. Russell [16] emphasized that metals under irradiation violate several conditions for equilibrium, and may attain a steady state that is not necessarily that of minimum free energy. He recommended an atomistic approach; i.e., using kinetic descriptions, and like Wilkes, attributed the low-temperature stability of the metastable amorphous state to slow crystallization relative to the mixing rate in displacement cascades.

Yang *et al.* [4] proposed that hcp $Zr(Fe,Cr)_2$ precipitates in Zircaloy serve as sinks for point defects during irradiation at reactor temperatures, and that amorphous transformation occurs when the defect density exceeds a critical value. They attributed the temperature dependence to a decrease in steady-state defect concentration with faster annealing at higher temperatures, and considered the loss of Fe to be a separate radiation-driven dissolution process. Griffiths *et al.* [5] also suggested that a competition between radiation damage to the lattice and thermally-driven recrystallization is operative at low temperatures. They concluded that progressive peripheral amorphous transformation at intermediate temperatures requires the introduction of hypostoichiometry by Fe depletion. Griffiths [12] later re-interpreted Yang's [6] directional-dissolution results with an earlier proposal [5] that Fe diffuses out of the precipitates after radiation excites Fe atoms into interstitial sites that are otherwise inaccessible.

Motta and Lemaignan [17] plotted the numerical tabular data from the work of Griffiths *et al.* [5], focusing on the marked linear relationship between amorphous-layer thickness and neutron fluence for temperatures between 523°K and 580°K. They acknowledged but ignored the flux dependence, and considered a departure from the $t^{1/2}$ dependence that normally characterizes thermally driven transport processes to be sufficient cause for rejecting rate-control by diffusion. Addressing only Zircaloy-4 precipitates in the database, they followed Griffiths *et al.* and suggested that an

irradiation-induced departure from stoichiometry is the rate-controlling mechanism for amorphization. Their ballistic mixing model predicts a linear dependence upon fluence, but contains no explicit dependence upon temperature, and does not explain the partially amorphous, non-depleted cores in Zircaloy-2 precipitates that show identical amorphous-layer behavior [5]. The many observations of amorphization at low temperatures, also without any change in stoichiometry, led Motta and Lemaignan to conclude that the amorphization mechanisms at intermediate and low temperatures are different.

A general acceptance of fluence as the key independent variable has made it difficult to quantify the effects of dose-rate on amorphization [18-21]. The corresponding implication that a crystalline lattice must sustain some critical amount of damage before transformation can occur has generated interest in both the temperature dependence of "dose-to-amorphization" and the "critical temperature for amorphization" [17,22,23]. The frequent observations of partial transformation prevent a precise definition of either quantity for the precipitates in Zircaloy. This paper offers an alternative approach, and suggests that treating flux and time as separate variables makes the unique crystalline-to-amorphous transformation of Zircaloy precipitates readily amenable to quantitative prediction.

DESCRIPTION OF THE MODEL

Conceptual Development – It is easiest to consider initially the $Zr(Fe,Cr)_2$ precipitates in Zircaloy-2. Their behavior [5,21] suggests that two separate processes control microstructural evolution as the phase transformation proceeds. First, a dynamic competition between flux-driven amorphization and thermally-driven recrystallization homogeneously converts a time-dependent fraction $\alpha(t)$ to the amorphous state. After sufficient time at constant flux ϕ and temperature T, the system attains a homogeneous steady-state amorphous fraction α_o that, in its extremes, approaches 1.0 (totally amorphous) for increasing ϕ / decreasing T, or remains close to 0.0 (crystalline) for decreasing ϕ / increasing T. Second, when the coefficient for thermal diffusion within the matrix is large enough to sustain the low end of a suitable activity gradient, Fe atoms diffuse through the amorphous portion of the precipitate to the matrix. Since diffusion outward from the core ceases upon removal of the neutron flux, and thermal annealing restores the original crystal structure by reversing the flow of Fe [6], outward diffusion requires energy from neutrons. The amorphous transformation apparently creates a metastable source of Fe atoms that is uniquely susceptible to mobilization by further excitation.

As the diffusion front moves into the precipitate, the composition of the new hypostoichiometric zone approaches a lower limit of about 10 at% Fe. This zone becomes, and remains, fully amorphous. The $Zr(Fe,Cr)_2$ precipitates in Zircaloy-4 resist homogeneous amorphizaton better than those in Zircaloy-2, and the hypostoichiometric structures transform easily. Apparently, the susceptibility of this pseudo-binary hcp Laves phase to loss of long-range order depends inversely upon the extent to which Fe replaces Cr in the lattice. The nature of the amorphous structure is not clear. It may be that the

neutron flux introduces Fe interstitialcies, and the resulting distortion at these lattice sites breaks or rotates bonds to form a macroscopically amorphous structure. Higher concentrations should make more Fe atoms available to reverse the damage and speed thermal recovery.

The Fe-depletion profiles within Zircaloy-2 $Zr(Fe,Cr)_2$ precipitates do not have the same step shape as those typical of the duplex crystalline/amorphous structures in Zircaloy-4 [21]. The latter reflect the sharp transition between a stable hcp lattice with its original composition, and the adjacent structure whose susceptibility to amorphization increases dramatically with small decreases in Fe content. The similar rates of amorphous-zone advancement in these different materials implies a comparable steady-state structure at the controlling interface. It is clear that maximum stability for the amorphous structure lies at about 10 at% Fe. The hcp $Zr(Fe_xCr_{1-x})_2$ structure is stable for $0.25 \leq x \leq 0.8$. When diffusion is slow relative to amorphization and recrystallization, the periphery of hcp structures with higher than optimum Fe approaches the composition of maximum stability. Those with lower than optimum Fe cannot recover. The Zircaloys behave as if that optimum occurs for $x \approx 0.5$, a composition typical for Zircaloy-2, accessible by loss of Fe to Zircaloy-4, and equidistant from the transitions to a cubic structure. In nomenclature from the Introduction, Fe-loss conversion of $Zr(Fe_{0.6}Cr_{0.4})_2$ to the micro-crystalline equivalent of hcp precipitates in Zircaloy-2 yields $(Zr_M)_{0.25} \bullet Zr(Fe_{0.5}Cr_{0.5})_2$, with Fe at 31 at%.

Energy Schematic – Although not strictly correct, it is useful to summarize these relationships in a schematic diagram that adds the high-energy metastable amorphous phase, its transition state, and the neutron flux to a thermodynamic description of the two stable phases. The shapes and relative positions of the free-energy curves in Figure 1 are consistent with non-equilibrium experimental observation, but for the most part represent materials with unknown structures. As a compromise, the composition axis uses at% for Fe content. The more structurally explicit Fe_x value is path-dependent, and inapplicable to the metal matrix.

A quantitative kinetic description of this system does not require intimate knowledge of the fast-neutron damage mechanisms or the amorphous microstructures. The key postulate is precipitate amorphization by the neutron excitation of Fe to a thermally inaccessible metastable state with a relatively small activation energy barrier in the reverse direction. The difference in energy between the intermediate transition state and the metastable amorphous state; i.e., the activation energy for recrystallization, also must increase as the concentration of Fe in the hcp lattice decreases.

After neutron excitation from susceptible sites that are specific to the amorphous structure, highly mobile Fe atoms become available for diffusion down an appropriate activity gradient through any structure with similar properties. Failure to dissipate a rapid accumulation of Fe in the matrix would slow, then stop further diffusion to that interface. Fe loss to 10 at% from $Zr(Fe_{0.5}Cr_{0.5})_2$ yields a micro-crystalline formula-equivalent of $(Zr_M)_{0.64} \bullet Zr(Fe_{0.18}Cr_{0.82})_2$, less matrix Zr than for Zircaloy-4, but a very similar lattice-Fe content that also coincides with the hexagonal-to-cubic transition. Transformation to a

more stable cubic lattice structure could prevent Fe depletion to less than 10 at%, but also would restore some crystallinity. It is more likely that a free-energy minimum within the hcp composition range prevents the amorphous composition from falling below 10 at%.

FORMULATION OF THE EQUATIONS

Amorphous Fraction α - The rate of change of the homogeneous amorphous fraction α is the difference between the rate of amorphization by the neutron flux ϕ, and the rate of thermal recrystallization. The extremely high kinetic energy of the neutrons (> 1 MeV) makes amorphization effectively independent of temperature. Recrystallization depends upon composition, but the model simplifies its description to that typical of $Zr(FeCr)_2$, and permits the use of a single rate constant with one pre-exponential factor and one activation energy. Thus

$$\mathbf{d\alpha/dt = k_\phi(1-\alpha)\phi - k_\chi\alpha \exp(-E^*/RT)} \qquad [1]$$

where k_ϕ, k_χ, and E* are constants. When the system reaches steady state at constant T and ϕ, $d\alpha/dt = 0$, $\alpha = \alpha_o$, and

$$\mathbf{\ln(\phi) = \ln(k_\chi/k_\phi) + \ln(\alpha_o/(1-\alpha_o)) - E^*/RT} \qquad [2]$$

The solution to Equation 1 for multiple intervals, each with a constant T and ϕ, is then

$$\alpha_n = \alpha_{o,n} - (\alpha_{o,n} - \alpha_{n-1}) \exp(-k_\phi\phi_n t_n/\alpha_{o,n}) \qquad [3]$$

or, for a single interval

$$\alpha = \alpha_o [1 - \exp(-k_\phi\phi t/\alpha_o)] \qquad [4]$$

Amorphous-Zone Thickness δ - There is insufficient information available for a rigorous description of Fe diffusion from the precipitate into the matrix, but the gradients are steep, and assuming short, constant diffusion distances is both simple and effective. Fe transport to the matrix-precipitate interface is proportional to the rate at which δ, the width of the amorphous zone, increases. If C_i is the concentration of diffusible Fe at that interface,

$$\mathbf{dC_i/dt = \gamma(d\delta/dt) - \varepsilon C_i} \qquad [5]$$

where ε is a temperature-dependent coefficient for diffusion into the matrix with effectively zero Fe concentration a short distance away. Fe diffusion from the central core defines the amorphous-zone growth rate, but mobility through the zone requires excitation by the neutron flux, and only the amorphous part of the core contains susceptible sites. Thus,

$$\mathbf{d\delta/dt = D\phi [\alpha(t) - \kappa C_i(t)]} \qquad [6]$$

where D is a temperature-independent coefficient for the flux-assisted diffusion of Fe within the amorphous zone, and κ is a normalizing constant. From Equations 5 and 6, $dC_i/dt = \gamma D\phi(\alpha-\kappa C_i) - \varepsilon C_i$. Solving yields an expression for $C_i(t)$ that, with Equation 4, makes possible a general solution of Equation 6 for $\delta(t)$.

At low temperatures, where ε approaches zero, essentially no Fe enters the matrix and the gradient across the amorphous zone disappears quickly. At intermediate temperatures, ε is non-zero and there is sufficient Fe diffusion into the matrix to sustain a gradient across the amorphous zone. There are no intervening data, and the intermediate-temperature data that are available show no evidence of diffusional temperature dependence. When ε is small and constant, C_i remains approximately proportional to δ, and making this assumption reduces the number of parameters. Diffusion is slow relative to amorphization, and replacing α with α_o simplifies the equations even further. For values of T, ϕ and t that are characteristic of commercial reactors,

$$\mathbf{d\delta/dt \approx D\phi(\alpha_o-\beta\delta)} \qquad [7]$$

where β is a normalizing constant, and

$$\mathbf{\delta = (\alpha_o/\beta)\,[1 - \exp(-\beta D\phi t)]} \qquad [8]$$

or

$$\mathbf{\delta_n = (\alpha_{o,n}/\beta)\,[1 - \exp(-\beta D\phi_n t_n)] + \delta_{n-1}\exp(-\beta D\phi_n t_n)} \qquad [9]$$

when T_n and ϕ_n remain constant during the n^{th} interval of length t_n.

ESTIMATION OF THE CONSTANTS

Data from Griffiths, Gilbert and Carpenter – Table 1 contains all the information on $Zr(Fe,Cr)_2$ precipitate amorphization from Table 1 of Reference 5, with additional columns for time and flux. The precision of the original dispacement-damage and fluence data warrants at most two significant figures, but the table retains three for clarity. The amorphous-layer thicknesses of the 3rd and 4th Dido specimens are the mathematical products of fluence and the original 20 nm/10^{25} n m^{-2} - estimate of their growth rate. A lack of internal consistency between the 2nd and 3rd BWR specimens suggests an error in fluence or dpa values, and the table addresses that possibility by considering one alternative.

Actvation Energy E* **-** According to Equation 2, a plot of $\ln(\phi)$ versus 1/T for constant α_o gives a line of slope –E*/R. The appearance of discernible transformation after very long times is readily identifiable experimentally, and is the only condition with both a high sensitivity to changes in ϕ and T, and a reproducible value of α_o.

Figure 2 includes all the data from Table 1. The challenge is to separate the almost-fully-crystalline from fully-crystalline precipitates when amorphous transformation of the latter may become discernable after longer times. The "iso-α_o" line in Figure 2 is a subjective compromise that yields

$$\mathbf{E^*/R = 11{,}600\ (°K)}$$

Kinetic Rate Constants k_ϕ and k_χ - Fitting Equation 8 to the data in Table 1 also requires $\ln(k_\chi/k_\phi)$. Assigning a value for α_o to the line in Figure 2 provides that, but the intercept is very sensitive to the choice when α_o approaches 0. The Zircaloy-2 553°K Dido specimens transformed partially to different, measurable degrees with a common α_o, and offer a unique opportunity to separate the rate constants with Equation 4. Griffiths *et al.* [5] described the central cores of these precipitates as "amorphous regions in a crystalline matrix" at $0.4\text{x}10^{25}$ n m^{-2}, and "crystalline regions in an amorphous matrix" at $2.0\text{x}10^{25}$ n m^{-2}. Values of 0.3 and 0.7 for α seemed consistent both with these descriptions, and with Figures 6(c) and 6(d) in Reference 5. The iterative solution of Equation 4 for these two specimens that share the same coordinates in Figure 2 is then

$$\mathbf{\alpha_o = 0.76} \qquad \mathbf{k_\phi = 9.6x10^{-22}\ cm^2\ n^{-1}}$$

and from Equation 2,

$$\mathbf{\ln(k_\chi/k_\phi) = 51.7} \qquad \mathbf{k_\chi = 27\ s^{-1}}$$

Time Constants – At low temperatures, the second term in Equation 1 is negligible, α is 0 initially, and

$$\mathbf{\alpha = 1 - \exp(-k_\phi \phi t)} \qquad \mathbf{\tau_\phi = (k_\phi \phi)^{-1}} \qquad \mathbf{[10]}$$

For $\phi = 1\text{x}10^{14}$ n cm^{-2} s^{-1}, τ_ϕ is $1\text{x}10^7$ s or about 120 days.

When the neutron flux vanishes at steady state, α decays from α_o as the precipitates recrystallize, and

$$\mathbf{\alpha = \alpha_o \exp[-k_\chi t \exp(-E^*/RT)]} \qquad \mathbf{\tau_\chi = [k_\chi \exp(-E^*/RT)]^{-1}} \qquad \mathbf{[11]}$$

At 560°K, τ_χ is $3.7\text{x}10^7$ s or about 425 days. It is clear that removing specimens for examination has essentially no effect on their in-pile morphology.

Flux-Assisted Diffusion Coefficient D and Normalizing Constant β - β links the concentration of mobile Fe to the degree of amorphization, and is not totally independent of D. The easiest way to include a contribution from each reactor was to select one specimen from the PHWR(CANDU), one from the BWR, and one from the PWR for determining the last two constants. The accuracy of the δ values is probably highest for

the widest amorphous zones, but the fluence data for the 40 nm BWR specimen seemed more reliable. The best fit to Equation 8 of those data, and the data from the 25 nm PHWR and 80 nm PWR specimens, occurred for

$$\beta = 2.37 \times 10^{-3}\ \text{nm}^{-1} \qquad D = 2.34 \times 10^{-20}\ \text{nm cm}^2\ \text{n}^{-1}$$

Consistency within the Database – Table 2 lists those specimens from Table 1 with measurable amorphous zones, the widths of those zones, and the predictions of Equations 2 and 8. Optimization among all the data might improve the fit, but the accuracy is sufficiently good to validate the simple model.

SUMMARY AND CONCLUSIONS

At intermediate temperatures, neutron radiation slowly transforms hcp Laves-phase $Zr(Fe,Cr)_2$ precipitates in Zircaloy-2 and Zircaloy-4 to an amorphous structure. The transformation starts at the periphery, and moves inward as Fe diffuses outward to the surrounding alloy matrix. With data from Reference 5, Figure 3 shows a general increase in the width of this amorphous zone with fluence, but the dependencies differ by up to a factor of two for comparable conditions in-pile. Simple kinetic equations that describe both the flux-assisted diffusion of Fe atoms, and a balance between amorphization and recrystallization, remove the inconsistency by making flux and time separate variables. The excellent correlation in Figure 4 supports a choice of 7×10^{13} n cm^{-2} as the fluence corresponding to 18 dpa in the BWR, or just twice the value in Table 1 for 9 dpa.

The steady-state and linear approximations proved adequate for the data in Reference 5. Equivalent accuracy requires both the time-dependent form of all equations at shorter intervals, and the transformation of the diffusion equation to spherical coordinates for amorphous zone widths approaching precipitate dimensions.

The temperature range was too narrow to quantify its effect on Fe diffusion into the alloy matrix. As a result, the simple model predicts a rate of Fe depletion and amorphous-zone growth that continues to increase with decreasing temperature because the homogeneous amorphous fraction α does so. At low temperatures, α approaches unity and no Fe leaves the precipitates. There should be a transition-temperature interval with precipitates that have both a low-Fe amorphous shell and a non-depleted amorphous core that careful analysis by transmission electron microscopy (TEM) could resolve. Table 1 contains no data for Zircaloy-4 precipitates below 560°K. At some lower temperature, partial amorphization of these more stable cores with higher Fe content and lower activation energy will become appreciable, and a single E* value will not suffice. Although the lack of TEM data at lower temperatures prevents generalization of the quantitative model, this simpler version accurately predicts Laves-phase precipitate amorphization in Zircaloy as a function of irradiation temperature, neutron flux, and exposure time for conditions typical of commercial power reactors. It should prove especially useful for investigating possible correlations with any Zircaloy characteristics that are measurable without destructive post-irradiation examination.

REFERENCES

[1] R.W. Gilbert, M. Griffiths and G.J.C. Carpenter, J. Nucl. Mater. 135 (1985) 265.

[2] W.J.S. Yang, R.P. Tucker, B. Cheng and R.B. Adamson, Proc. Workshop on Second Phase Particles and Matrix Properties of the Zircaloys, Erlangen, 1985.

[3] M. Griffiths, R.W. Gilbert and B.A. Cheadle, *ibid.*

[4] W.J.S. Yang, R.P. Tucker, B. Cheng and R.B. Adamson, J. Nucl. Mater. 138 (1986) 185.

[5] M. Griffiths, R.W. Gilbert and G.J.C. Carpenter, J. Nucl. Mater. 150 (1987) 53.

[6] W.J.S. Yang, J. Nucl. Mater. 158 (1988) 71.

[7] D. Shaltiel, I. Jacob and D. Davidov, J. Less-Common Metals 53 (1977) 117.

[8] W.J.S. Yang and R.B. Adamson, Proc. 8th Intl. Symp. on Zirconium in the Nuclear Industry, ASTM STP 1023 (1989) 451.

[9] V.K. Sinha, G.Y. Yu and W.E. Wallace, J. Less-Common Metals 106 (1985) 67.

[10] J.B. Van der Sande and A.L. Bement, J. Nucl. Mater. 52 (1974) 115.

[11] P. Chemelle, D.B. Knorr, J.B. Van der Sande and R.M. Pelloux, J. Nucl. Mater. 113 (1983) 58.

[12] M. Griffiths, J. Nucl. Mater. 170 (1990) 294.

[13] F. Garzarolli, P. Dewes, G. Maussner and H.-H. Basso, Proc. 8th Intl. Symp. on Zirconium in the Nuclear Industry, ASTM STP 1023 (1989) 641.

[14] E.M. Schulson, J. Nucl. Mater. 83 (1979) 239.

[15] P. Wilkes, J. Nucl. Mater. 83 (1979) 166.

[16] K.C. Russell, J. Nucl. Mater. 83 (1979) 176.

[17] A.T. Motta and C. Lemaignan, J. Nucl. Mater. 195 (1992) 277.

[18] B.-C. Cheng, R.M. Kruger and R.B. Adamson, Proc. 10th Intl. Symp. on Zirconium in the Nuclear Industry, ASTM STP 1245 (1994) 400.

[19] D. Gilbon and C. Simonot, Proc. 10th Intl. Symp. on Zirconium in the Nuclear Industry, ASTM STP 1245 (1994) 521.

[20] F. Garzarolli, W. Goll, A. Seibold and I. Ray, Proc. 11th Intl. Symp. on Zirconium in the Nuclear Industry, ASTM STP 1295 (1996) 541.

[21] M. Griffiths, J.F. Mecke and J.E. Winegar, Proc. 11th Intl. Symp. on Zirconium in the Nuclear Industry, ASTM STP 1295 (1996) 580.

[22] A.T. Motta, F. Lefebvre and C. Lemaignan, Proc. 9th Intl. Symp. on Zirconium in the Nuclear Industry, ASTM STP 1132 (1991) 718.

[23] A.T. Motta, J. Nucl. Mater. 244 (1997) 227.

FIGURE CAPTIONS

Figure 1. Schematic Pseudo-Free-Energy Diagram for Amorphization of Laves-Phase Precipitates in the Zircaloys during Neutron Irradiation. The neutron flux drives Fe atoms in the hcp lattice over a very high energy barrier into a metastable amorphous state. Thermal activation restores crystallinity when the temperature is high enough to overcome the relatively small, composition-dependent barrier in the reverse direction. At low temperatures, the transformation is rapid and complete. At high temperatures, the precipitates remain crystalline. The flux mobilizes Fe atoms that occupy amorphous-specific sites and diffuse to the matrix until Fe build-up at that interface renders the activity gradient ineffective. Minima in free energy drive the amorphous and crystalline states toward 10 and 33 at% Fe, respectively. At intermediate temperatures, outward diffusion leaves the perimeter of crystalline $Zr(Fe_{0.6}Cr_{0.4})_2$ in Zircaloy-4 behaving like the more susceptible, partially amorphous $Zr(FeCr)_2$ in Zircaloy-2, and both types of precipitates develop a peripheral amorphous zone that approaches 10 at% Fe.

Figure 2. Activation-Energy Plot of Amorphization Data from Table 1. Open symbols represent fully amorphous $Zr(Fe,Cr)_2$ precipitates; closed, fully crystalline; combination symbols, a duplex structure. The best choice for an "iso-α_o" line is an estimate of those coordinates that represent minimal, but discernible transformation after very long times.

Figure 3. Dependence of Amorphous-Zone Width upon Fluence. Data from Table 1 for temperatures between 523°K and 580°K with a fluence of $7x10^{21}$n cm^{-2} at 18 dpa in the BWR.

Figure 4. Internal Consistency of the Steady-State Model. Data from Table 2 with a flux of $6.2x10^{13}$n $cm^{-2}s^{-1}$ for a zone width of 90nm in the BWR (fluence of $7x10^{21}$n cm^{-2} at 18 dpa). The line passes through the origin with unit slope.

TABLES

Table 1. Amorphization Data for $Zr(Fe,Cr)_2$ from Griffiths *et al* [5]

Alloy	Reactor	Damage (dpa/s)	Damage (dpa)	Time (s)	Fluence (n/cm^2)	Flux (n/cm^2-s)	Temp (K)	Structure
Zcly-2	Dido	1.10E-07	1.5	1.36E+07	6.00E+20	4.40E+13	353	Amorphous
			6	5.45E+07	2.50E+21	4.58E+13		Amorphous
		1.70E-07	1	5.88E+06	4.00E+20	6.80E+13	553	Duplex(8nm)
			5	2.94E+07	2.00E+21	6.80E+13		Duplex(40nm)
	CANDU	1.00E-08	2	2.00E+08	1.00E+21	5.00E+12	350	Amorphous
		4.00E-08	12.5	3.13E+08	6.00E+21	1.92E+13		Amorphous
		5.00E-09	1	2.00E+08	5.00E+20	2.50E+12	523	Crystalline
		6.00E-09	2	3.33E+08	9.00E+20	2.70E+12		Duplex(10nm)
		1.50E-08	4	2.67E+08	2.10E+21	7.88E+12		Duplex(25nm)
		5.00E-08	15	3.00E+08	7.20E+21	2.40E+13	550	Amorphous
	EBR-II	8.00E-07	20	2.50E+07	6.20E+21	2.48E+14	675	Crystalline
Zcly-4	BWR	1.50E-08	2	1.33E+08	1.00E+21	7.50E+12	560	Duplex(10nm)
		8.00E-08	9	1.13E+08	3.50E+21	3.11E+13		Duplex(40nm)
		1.60E-07	18	1.13E+08	8.50E+21	7.56E+13		Duplex(90nm)
					7.00E+21	6.22E+13		
	PWR	1.00E-08	1	1.00E+08	5.00E+20	5.00E+12	580	Crystalline
		1.60E-07	18	1.13E+08	8.00E+21	7.11E+13		Duplex(80nm)

Table 2. Predictions of the Model

Alloy	Reactor	Zone Width Observed (nm)	Zone Width Predicted (nm)
Zcly-2	Dido	8	7.0
		40	33.6
	CANDU	10	6.0
		25	25.3
Zcly-4	BWR	10	4.8
		40	38.9
		90	115.3
	(alternate flux)		93.3
	PWR	0	0.9
		80	83.3

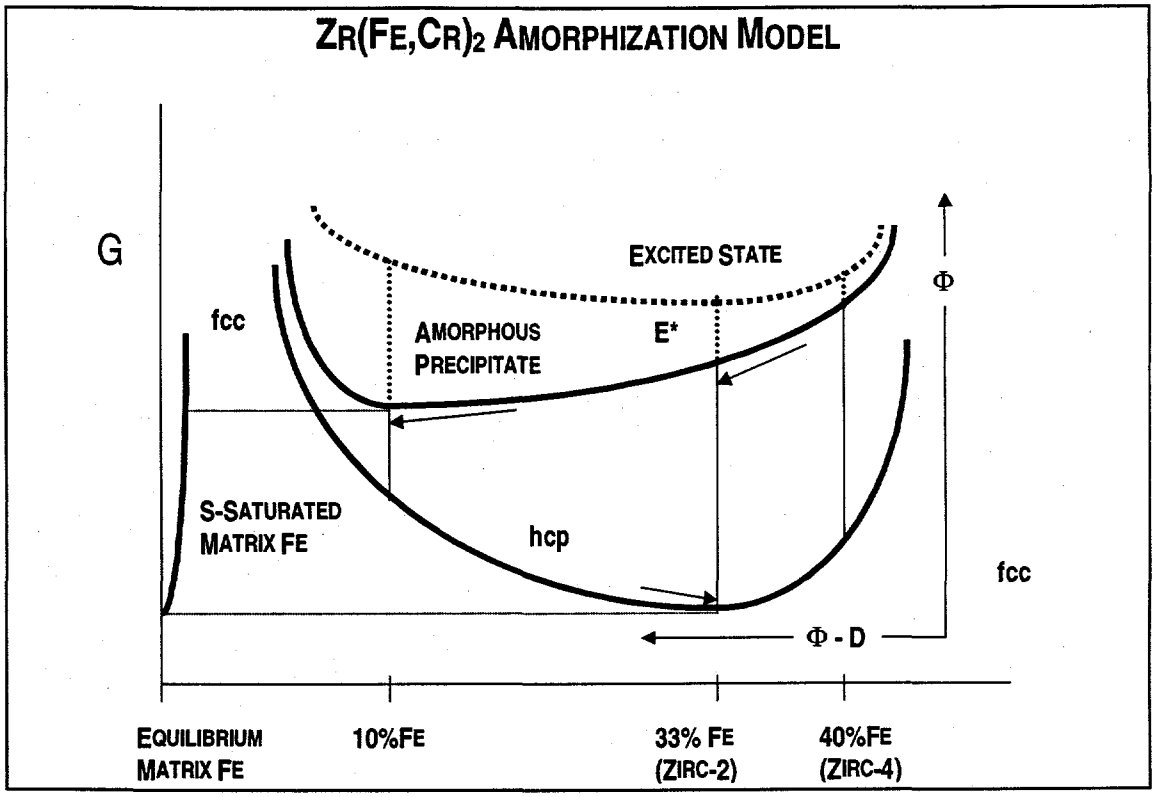

Figure 1. Schematic Pseudo-Free-Energy Diagram for Amorphization of Laves-Phase Precipitates in the Zircaloys during Neutron Irradiation. The neutron flux drives Fe atoms in the hcp lattice over a very high energy barrier into a metastable amorphous state. Thermal activation restores crystallinity when the temperature is high enough to overcome the relatively small, composition-dependent barrier in the reverse direction. At low temperatures, the transformation is rapid and complete. At high temperatures, the precipitates remain crystalline. The flux mobilizes Fe atoms that occupy amorphous-specific sites and diffuse to the matrix until Fe build-up at that interface renders the activity gradient ineffective. Minima in free energy drive the amorphous and crystalline states toward 10 and 33 at% Fe, respectively. At intermediate temperatures, outward diffusion leaves the perimeter of crystalline $Zr(Fe_{0.6}Cr_{0.4})_2$ in Zircaloy-4 behaving like the more susceptible, partially amorphous $Zr(FeCr)_2$ in Zircaloy-2, and both types of precipitates develop a peripheral amorphous zone that approaches 10 at% Fe.

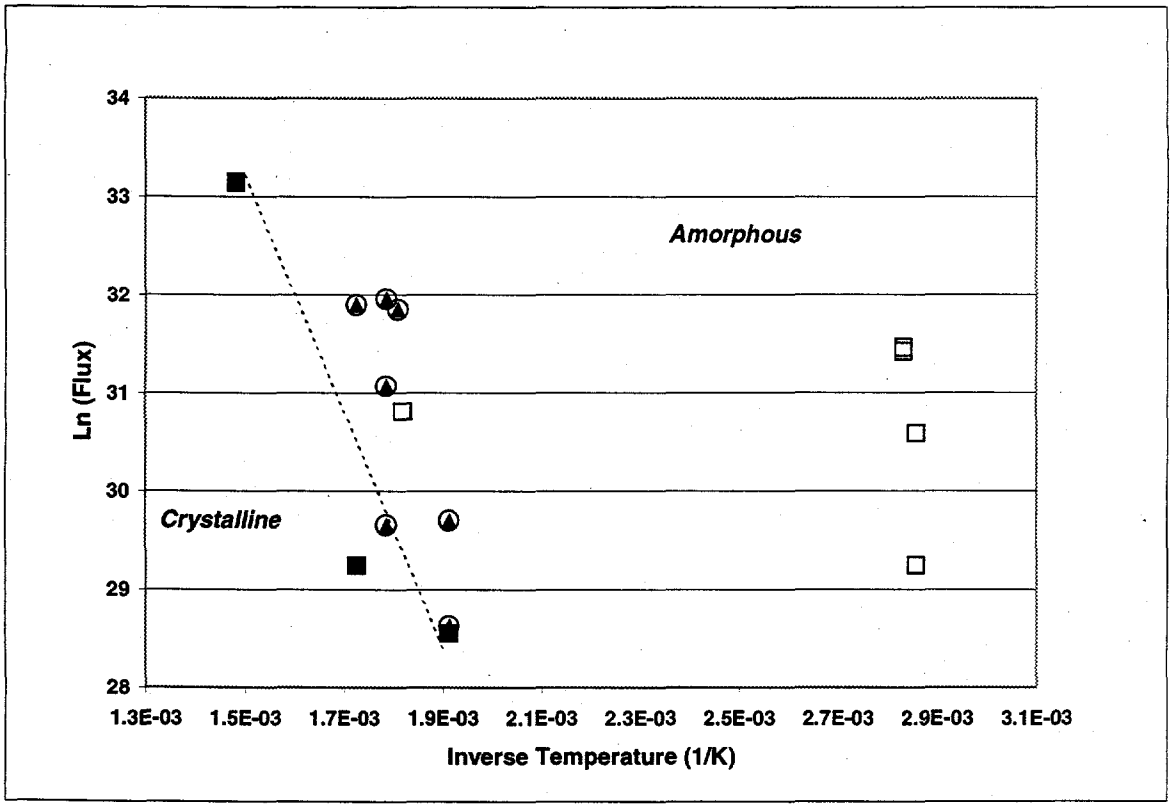

Figure 2. Activation-Energy Plot of Amorphization Data from Table 1. Open symbols represent fully amorphous $Zr(Fe,Cr)_2$ precipitates; closed, fully crystalline; combination symbols, a duplex structure. The best choice for an "iso-α_o" line is an estimate of those coordinates that represent minimal, but discernible transformation after very long times.

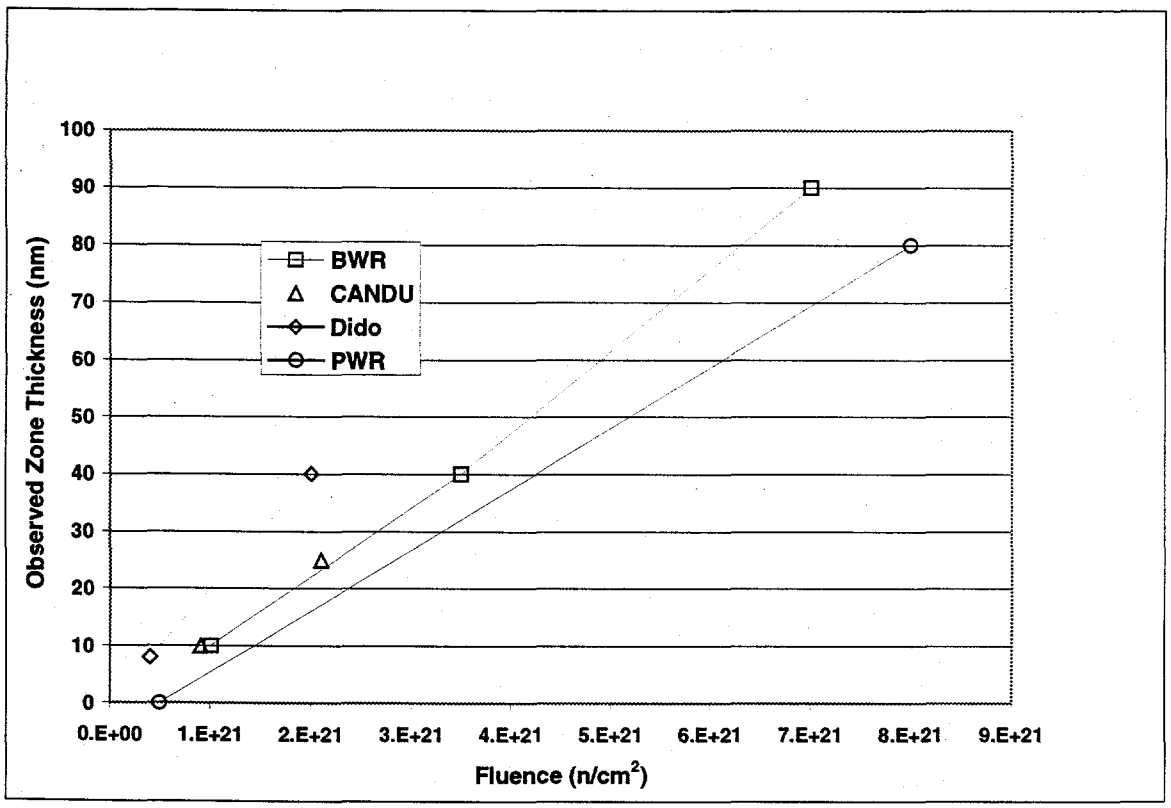

Figure 3. Dependence of Amorphous-Zone Width upon Fluence. Data from Table 1 for temperatures between 523°K and 580°K with a fluence of $7x10^{21}$n cm^{-2} at 18 dpa in the BWR.

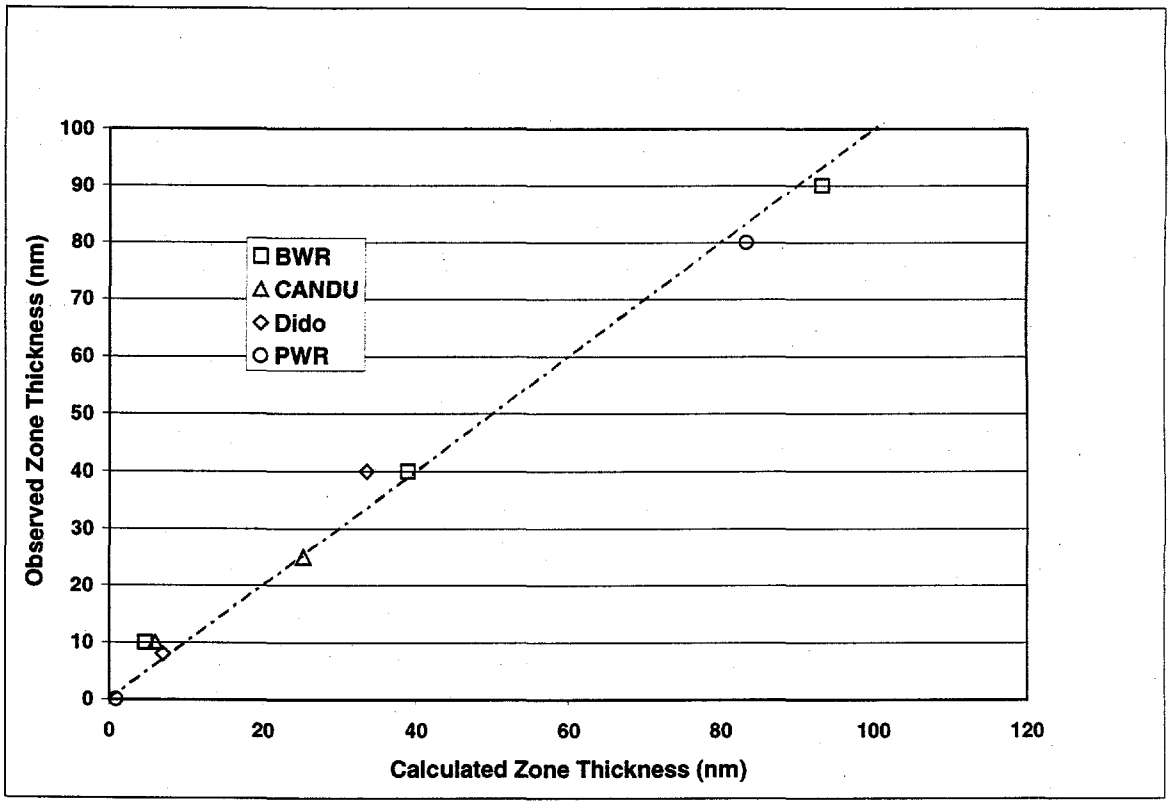

Figure 4. Internal Consistency of the Steady-State Model. Data from Table 2 with a flux of 6.2×10^{13}n $cm^{-2}s^{-1}$ for a zone width of 90nm in the BWR (fluence of 7×10^{21}n cm^{-2} at 18 dpa). The line passes through the origin with unit slope.